Molecular Dynamics of the Interaction of Some Alkaline-Earth Cations with Some Pentoses Undergoing $4C_1 \rightleftharpoons 1C_4$ Isomerization

Sergio Petrucci*,† and Edward M. Eyring‡

Polytechnic University, Long Island Center, Farmingdale, New York 11735, and Department of Chemistry, University of Utah, Salt Lake City, Utah 84112

Received: March 12, 2002; In Final Form: July 17, 2002

Ultrasonic relaxation spectra in the frequency range 0.08−400 MHz of the ions Ca^{2+} or Ba^{2+}, interacting with the pentoses D-(−)-ribose, D-(−)-lyxose, and D-(−)-arabinose at concentrations of 0.5 M and molar ratio (pentose/metal^{2+}) = 1 at 25 °C, are reported. For Ca^{2+} or Ba^{2+} with D-(−)-ribose ultrasonic relaxation spectra at various concentrations up to $c = 0.7$ mol/dm^3 at 25 °C are also reported. The ultrasonic spectra can be interpreted by the sum of three Debye relaxation processes. The one at the lowest relaxation frequency (∼0.07−0.25 MHz) is ascribed to the $4C_1 \rightleftharpoons 1C_4$ isomerization of the carbohydrates. The relaxation process at intermediate frequency (∼10−12 MHz for Ca^{2+} *or* 50−60 MHz for Ba^{2+}) is interpreted as due to the partial desolvation of the cations by the carbohydrate. The "fast" relaxation process at 120−160 MHz is attributed to the diffusion-controlled approach and initial desolvation of the cation and carbohydrate. The two faster processes are interpreted according to the multistep Eigen−Tamm complexation mechanism: M^{2+} + carbohydrate $\leftrightarrows$ (k_1/k_{-1}) $M^{2+}\cdots$carbohydrate $\leftrightarrows$ (k_2/k_{-2}) M^{2+} carbohydrate.

Introduction

The molecular relaxation dynamics of Ca^{2+} and Ba^{2+} added to glucose, at a concentration ratio $R \cong 1$, have been reported[1] and interpreted by a multistep Eigen−Tamm mechanism.[2] For the case of glucose, the rotation of the CH_2–OH group of the C-6 carbon was a complication, and the unobservability of a $4C_1 \rightleftharpoons 1C_4$ equilibrium, because of the excess of one of the two forms, deprived the research of the presence of a detectable ∼0.1 MHz process[3] and of the possible elucidation of the influence of the cations on the $4C_1 \rightleftharpoons 1C_4$ isomeric relaxation. For the nonspecialist reader, the $4C_1 \rightleftharpoons 1C_4$ symbolism refers to the process illustrated below, where the numbers identify the upper or lower position of the carbon atoms 4 or 1 of the carbohydrate ring with respect to the plane passing through the carbon atoms 2, 3, and 5 and the oxygen atom of the ring.

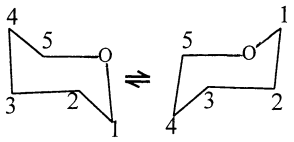

For the pentoses D-(−)-ribose, D-(−)-lyxose, and D-(−)-arabinose, the presence of both $4C_1$ and $1C_4$ conformations, at comparable concentrations, has been established,[3] and the dynamics of the process $4C_1 \rightleftharpoons 1C_4$ (or of its reverse) have been studied, by ultrasonic relaxation spectra as reported before,[3] in the frequency range 0.10−2000 MHz. It was then logical to extend this study to the molecular interaction of either Ca^{2+} or Ba^{2+} with the above pentoses.

Experimental Section

The resonator cells[4] and technique[4] and the pulse technique[5] have been described previously. A new ultrasonic resonator cell has been used in the frequency range ∼80−1100 kHz (0.08−1.1 MHz). The cell, holding a ∼40 cm^3 volume of liquid is equipped with concave, X-cut, 1.25 MHz fundamental quartz crystals that were cut and made concave by Mr. W. Sauermann of the Max Planck Institute of Nikolausberg, Germany. The radius of curvature of the crystals was 2.0 m. The crystals were gold plated, coaxially on the convex contact side, and were gold plated on the edges and on the concave side. With a rubber ring of about 8 mm thickness, separating the two crystals, resonances separated by about 60 kHz were recorded between 80 kHz and ∼1.1 MHz. The cell was calibrated with a 0.20 M $MnSO_4$ solution in water at 25 °C, leading to results consistent with those of Hemmes et al.,[5] obtained in our laboratory by the pulse technique in the frequency range 3−350 MHz.

The reagents, D-(−)-ribose (Fluka, >99%), D-(−)-lyxose (Sigma, minimum 99%), and D-(−)-arabinose (Sigma, minimum 99%), were used as received. $CaCl_2 \cdot 2H_2O$ and $Ba(ClO_4)_2$ were Aldrich products, 98% and 99% pure, respectively. They were kept in desiccators and weighed in a drybox together with the pentoses in volumetric flasks. Deionized water was added, up to the fiduciary mark, after the salts and pentoses had dissolved in the partially filled flasks. The solutions were kept in a refrigerator for at least 1 day before use. No solution was used more than 3 days after its preparation.

Results and Calculations

Figure 1 reports the ultrasonic spectrum for 0.50 M D-(−)-ribose in the form of α/f^2 vs the frequency f (∼0.1 to ∼400 MHz) at 25 °C. The solid line for the "solvent", at this concentration, interprets the data by the Debye function for a single relaxation frequency f_{111} according to the function:[6]

$$\frac{\alpha}{f^2} = \frac{A_{111}}{1 + (f/f_{111})^2} + B \qquad \text{(I)}$$

† Polytechnic University.
‡ University of Utah.

10.1021/jp0206875 CCC: $22.00
Published on Web 08/31/2002

TABLE 1: Ultrasonic Parameters A_1, f_1, A_{11}, f_{11}, A_{111}, f_{111}, and B, and Sound Velocities u, According to the Fitted Function (eq I) for All the Systems Investigated at 25 °C

c^a (mol/dm^3)	$A_1 \times 10^{17}$ (cm^{-1} s^2)	f_1 (MHz)	$A_{11} \times 10^{17}$ (cm^{-1} s^2)	f_{11} (MHz)	$A_{111} \times 10^{17}$ (cm^{-1} s^2)	f_{111} (MHz)	$B \times 10^{17}$ (cm^{-1} s^2)	$u \times 10^{-5}$ (cm s^{-1})
System: Ca^{2+} + D-(−)-Ribose								
0.70	11	170	525	12	42 000	0.10	22	1.589
0.50	8	150	300	10	30 000	0.22	23	1.562
0.35	5	140	220	10	18 000	0.15	22	1.537
0.25	5	140	162	10	15 000	0.25	18	1.543
0 (0.50 M ribose)					9 000	0.25	24	1.547
System: Ca^{2+} + D-(−)-Lyxose								
0.50	10	150	60	10	52 000	0.09	21	1.569
0 (0.50 M lyxose)					52 000	0.09	22.5	1.515
System: Ca^{2+} + D-(−)-Arabinose								
0.50	10	150	70	10	14 000	0.18	23	1.563
0 (0.40 M arabinose)					39 700	0.20	22	1.511
System: Ba^{2+} + D-(−)-Ribose								
0.50	40	150	40	60	130 000	0.07	22	1.512
0.35	28	145	28	55	40 000	0.15	23	1.512
0.25	20	130	20	55	60 000	0.09	22	1.516
0.15	11	120	11	50	27 000	0.15	22	1.507
System: Ba^{2+} + D-(−)-Lyxose								
0.50	12	150	22	60	30 000	0.09	22	1.515
System: Ba^{2+} + D-(−)-Arabinose								
0.50	6.6	150	6	60	46 000	0.10	24	1.524

[a] Molar ratio [M^{2+}]/[carbohydrate] = 1.

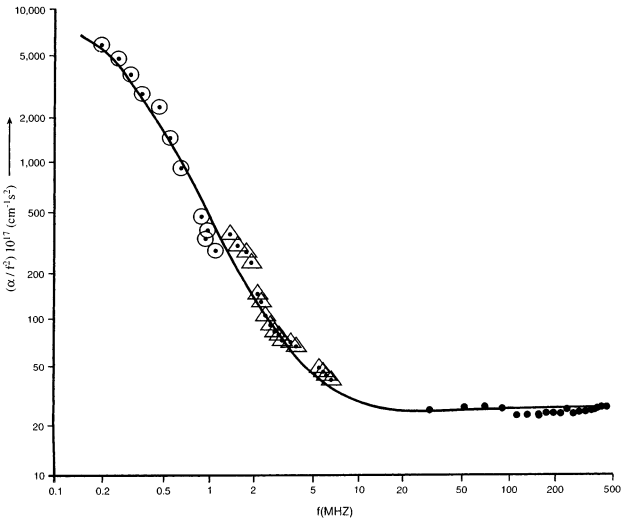

Figure 1. Ultrasonic spectrum, in the form (α/f^2) vs frequency f, for the system D-(−)-ribose at concentration $c = 0.50$ mol/dm^3 in water at 25 °C.

α is the sound absorption coefficient (neper/cm = 1/8.686 decibel/cm) at the frequency f. For a nonrelaxing fluid, α is proportional to f^2. Thus a plot of α/f^2 versus f as in Figure 1 should be a horizontal straight line in the absence of a relaxation process. When a relaxation process is present, energy absorbed by the molecular process responsible (partially) for the value of α decreases with increasing f (because that particular relaxation process occurs less and less with increasing f). Hence the frequency normalized value of α, expressed by the ratio α/f^2, undergoes a descending sigmoid behavior with increasing f that tends to the constant value of α/f^2 at higher frequencies corresponding to the remaining nonrelaxed processes in the fluid. A_{111} contains the relaxation information due to the observed process. B is the value of α/f^2 for frequencies much larger than f_{111}. When there are multiple Debye processes, as in the present case, characterized by relaxation frequencies f_1, f_{11}, ..., f_n, the above sequence repeats itself each time the increasing frequency f approaches one of the relaxation frequencies.

Sound absorption data are sometimes plotted[3] in terms of the excess sound absorption coefficient α_{exc} as the quantity

$$\mu \equiv \alpha_{exc}\lambda = \left(\frac{\alpha}{f^2} - B\right)uf \qquad \text{(II)}$$

versus frequency f. Here u denotes the sound velocity and λ the wavelength of sound; i.e., $u = \lambda f$. A μ versus f plot of ultrasonic data is sometimes preferred because the broad maxima resemble other types of absorption spectra.

Notice that small effects centered at 20−50 MHz reported before[3] for concentrations ≥1 M are not discernible in Figure 1. A single Debye process seems to interpret the data adequately. Table 1 reports the parameters A_{111}, f_{111}, and B for the "solvent" 0.50 M D-(−)-ribose in water and 25 °C. (The subscript "111" is intended to emphasize comparison with the electrolyte solutions below.)

Figure 2 shows the ultrasonic spectrum of 0.50 M Ca^{2+} + 0.50 M D-(−)-ribose in the form of α/f^2 vs the frequency f (∼0.1 to ∼400 MHz) at 25 °C. The sound absorption spectrum of Figure 2 appears more complex than that of Figure 1 with the slowest relaxation process enhanced. The spectrum profile can be interpreted as the sum of three Debye relaxation processes characterized by the relaxation frequencies f_1, f_{11}, and f_{111}, according to the function of eq I:[6]

$$\frac{\alpha}{f^2} = \frac{A_1}{1 + (f/f_1)^2} + \frac{A_{11}}{1 + (f/f_{11})^2} + \frac{A_{111}}{1 + (f/f_{111})^2} + B \qquad \text{(III)}$$

where A_1, A_{11}, and A_{111} contain the information associated with the three relaxation processes, whereas B is the value of α/f^2 at frequencies much above f_1, f_{11}, and f_{111}, namely the high-frequency background absorption function $(\alpha/f^2)_{f \gg f_1, f_{11}, f_{111}}$.

Figure 3 shows the ultrasonic spectrum of 0.50 M D-(−)-lyxose in the form of (α/f^2) vs the frequency f (∼0.1 to ∼400 MHz) at 25 °C. Table 1 reports the parameters used according

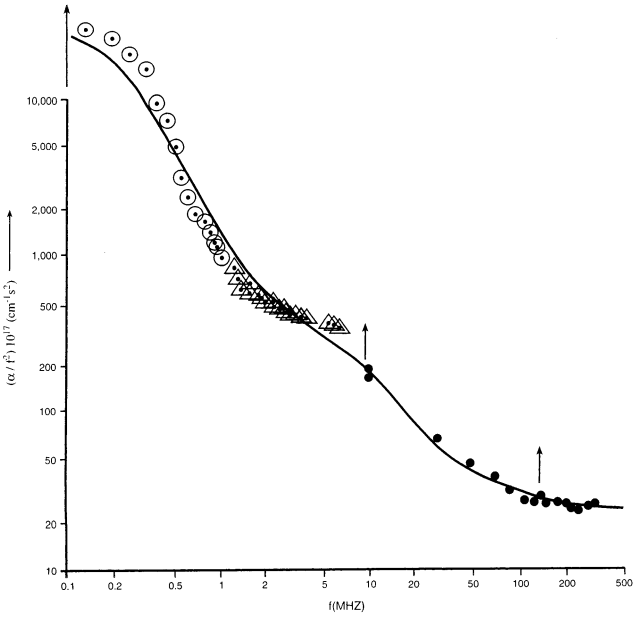

Figure 2. Ultrasonic spectrum, in the form (α/f^2) vs frequency f, for the system Ca^{2+} + D-(−)-ribose at concentration $c = 0.50$ *mol/dm³, molar ratio ([Ca²⁺]/[D-(−)-ribose]) = 1, and temperature 25 °C.*

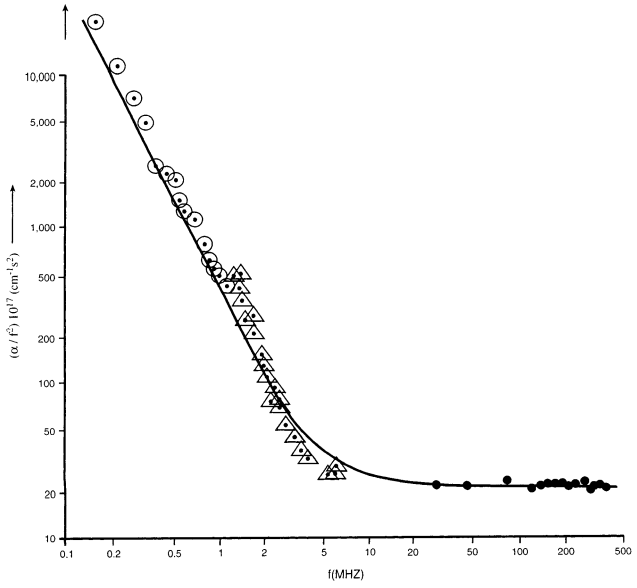

Figure 3. Ultrasonic spectrum, in the form (α/f^2) vs frequency f, for the system D-(−)-lyxose at concentration $c = 0.50$ mol/dm³ in water at 25 °C.

to eq I to fit the data in accord with a single Debye relaxation function which is also adequate in this case.

Figure 4 shows the ultrasonic spectrum of Ba^{2+} 0.50M + D-(−)-lyxose 0.50M in the form of α/f^2 vs the frequency f (~0.1 to ~400 MHz) at 25 °C. For this representative spectrum as well as for all those investigated in this work, the spectrum profile for the solutions of electrolytes can be interpreted as the sum of three Debye relaxation processes, characterized by the relaxation frequencies f_1, f_{111} and f_{111}, according to the function of eq III.[6]

Table 1 contains the parameters A_1, f_1, A_{11}, f_{11}, A_{111}, f_{111}, and B and the measured sound velocity u (cm/s) for all the concentrations and pentoses investigated at 25 °C.

Scrutiny of the results indicates that the relaxation frequency f_1 is fairly independent of the nature of the cation and of the pentose considered. Further, f_{11} seems to be ~10 MHz for Ca^{2+}

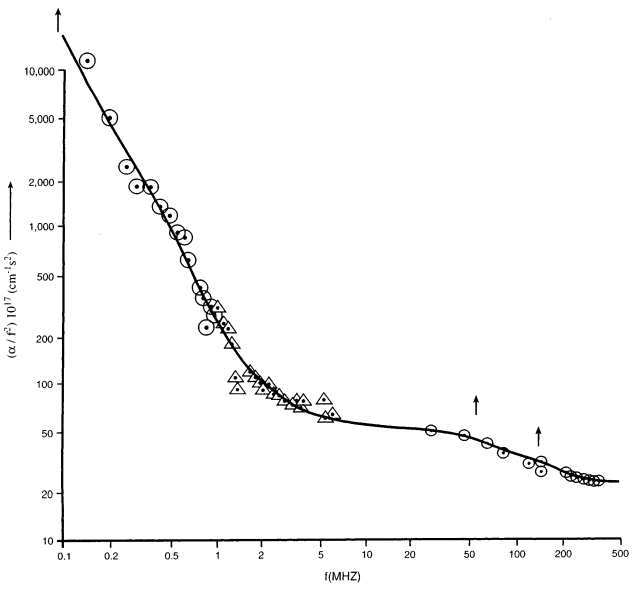

Figure 4. Ultrasonic spectrum, in the form (α/f^2) vs frequency f, for the system Ba^{2+} + D-(−)-lyxose at the concentration $c = 0.50$ mol/dm³, molar ratio ([Ba^{2+}]/[D-(−)-lyxose] = 1, and temperature 25 °C.

and ~60 MHz for Ba^{2+}; namely, the ratio $f_{11}(Ba^{2+})/f_{11}(Ca^{2+}) \approx 6$. Textbooks[7] report the rate constant of substitution of the first coordination sphere water around the cations Ba^{2+} and Ca^{2+} to be about 1 order of magnitude apart, namely $k(Ba^{2+})/k(Ca^{2+}) \approx 10$. The above considerations suggest that the processes characterized by f_1 and f_{11} correspond to the Eigen−Tamm complexation scheme.

$$M^{2+} + \text{carbohydrate} \underset{k_{-1}}{\overset{k_1}{\rightleftharpoons}} M^{2+}\cdots\text{carbohydrate} \underset{k_{-2}}{\overset{k_2}{\rightleftharpoons}} (M^{2+}\ \text{carbohydrate}) \quad \text{(IV)}$$

with $M^{2+}\cdots$carbohydrate denoting a solvent separated species, whereas (M^{2+} carbohydrate) is the contact metal ion−carbohydrate complex.

The relaxation process characterized by the relaxation frequency f_{111} is attributed to the isomeric ring inversion $4C_1 \rightleftharpoons 1C_4$, a process already studied separately.[3] Unfortunately, limitation of our lowest accessible frequency to ~80 kHz (0.08 MHz) precludes a precise determination of any possible effect of the complexed cations on f_{111} that, therefore, must be retained in a semiqualitative way, as a figure of approximate value.

More relevant, for the present work, is the study of the concentration dependence of process IV which has been carried out for both Ca^{2+} + D-(−)-ribose and Ba^{2+} + D-(−)-ribose at 25 °C.

The Eigen−Tamm matrix analysis of process IV leads, for the position k_1, $k_{-1} \gg k_2$, k_{-2}, to the expressions[6]

$$\tau_I^{-1} = 2\pi f_1 = k_1\theta + k_{-1} \quad \text{(V)}$$

$$\tau_{II}^{-1} = 2\pi f_{11} = k_2\frac{\theta}{\theta + K_{-1}} + k_{-2} \quad \text{(VI)}$$

with $\theta = 2\sigma c$, where σ is the degree of dissociation of the complexes Ca^{2+}−ribose *or* Ba^{2+}−ribose and $K_{-1} = k_{-1}/k_1$. The quotient $\theta/(\theta + K_{-1})$ in (VI) is denoted hereafter by ϕ.

Stability constants $K = [M^{2+}\text{−ribose}]/[M^{2+}][\text{ribose}]$, omitting ionic activity coefficient ratios, namely stoichiometric stability constants for Ca^{2+}−ribose and Ba^{2+}−ribose, were reported[8] to

TABLE 2: Calculated σ, θ, and ϕ Values at the Concentrations Investigated for Ca^{2+} + D-(−)-Ribose and Ba^{2+} + D-(−)-Ribose at 25 °C[a]

System: Ca^{2+} + D-(−)-Ribose, 25 °C[b]

c (mol/dm^3)	σ[c]	$\theta = 2\sigma c$	$\tau_I^{-1} = 2\pi f_{1,}$ s^{-1}	$\phi = \theta/(\theta + K_{-1})$	$\tau_{II}^{-1} = 2\pi f_{11,}$ s^{-1}
0.70	0.5986	0.8381	1.07×10^9	0.3423	7.5×10^7
0.50	0.6559	0.6559	0.94×10^9	0.2895	6.3×10^7
0.35	0.7143	0.500	0.88×10^9	0.2370	6.3×10^7
0.25	0.7656	0.383	0.88×10^9	0.1922	6.3×10^7

System: Ba^{2+} + D-(−)-Ribose, 25 °C[d]

c (mol/dm^3)	σ[e]	$\theta = 2\sigma c$	$\tau_I^{-1} = 2\pi f_{1,}$ s^{-1}	$\phi = \theta/(\theta + K_{-1})$	$\tau_{II}^{-1} = 2\pi f_{11,}$ s^{-1}
0.50	0.6457	0.6457	0.94×10^9	0.3353	3.8×10^8
0.35	0.7046	0.4932	0.91×10^9	0.2781	3.5×10^8
0.25	0.7567	0.2784	0.82×10^9	0.2282	3.5×10^8
0.15	0.8260	0.2478	0.75×10^9	0.1622	3.1×10^8

[a] The quantities τ_I^{-1} and τ_{II}^{-1}, the inverse of the "fast" and "slow" relaxation times, are reported together with the results for rate constant and equilibrium constants. [b] Linear regression of τ_I^{-1} vs θ: $r^2 = 0.89$; intercept $= k_{-1} = 6.9 \times 10^8$ s^{-1}; slope $= k_1 = 4.3 \times 10^8$ M^{-1} s^{-1}; $K_1 = (k_1/k_{-1}) = 0.62$. Linear regression τ_{II}^{-1} vs ϕ: $r^2 = 0.63$; intercept $= k_{-2} = 4.7 \times 10^7$ s^{-1}; slope $= k_2 = 7.3 \times 10^7$ s^{-1}; $K_2 = (k_2/k_{-2}) = 1.6$; $K = K_1(1 + K_2) = 1.6$. [c] From $K = 1.6 = (1 - \sigma)/\sigma^2 c$. [d] Linear regression of τ_I^{-1} vs θ: $r^2 = 0.95$; intercept $= k_{-1} = 6.4 \times 10^8$ s^{-1}; slope $= k_1 = 5.0 \times 10^8$ M^{-1} s^{-1}; $K_1 = (k_1/k_{-1}) = 0.7_8$. Linear regression of τ_{II}^{-1} vs ϕ: $r^2 = 0.92$; intercept $= k_{-2} = 2.6 \times 10^8$ s^{-1}; slope $= k_2 = 3.4 \times 10^8$ s^{-1}; $K_2 = (k_2/k_{-2}) = 1.3$; $K = K_1(1 + K_2) = 1.8$. [e] From $K = 1.7 = (1 - \sigma)/\sigma^2 c$.

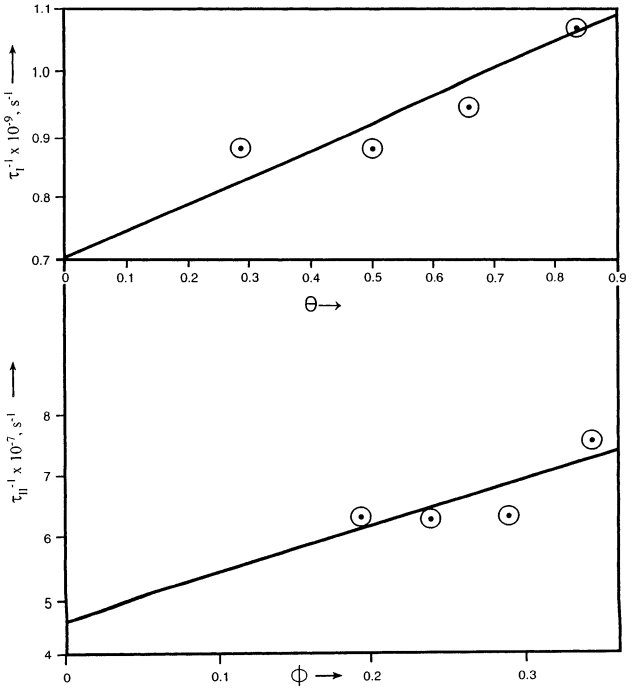

Figure 5. (a, top) Plot of τ_I^{-1} vs θ for Ca^{2+} + D-(−)-ribose at 25 °C. (b, bottom)Plot of τ_{II}^{-1} vs $\phi = \theta/(\theta + K_{-1})$, for Ca^{2+} + D-(−)-ribose at 25 °C.

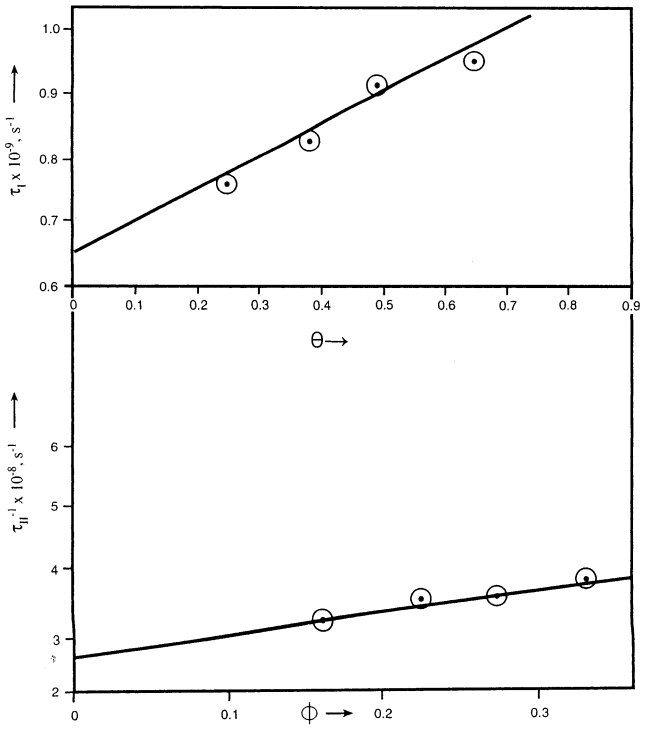

Figure 6. (a, top) Plot of τ_I^{-1} vs θ for Ba^{2+} + D-(−)-ribose at 25 °C. (b, bottom) Plot of τ_{II}^{-1} vs $\phi = \theta/(\theta + K_{-1})$, for Ba^{2+} + D-(−)-ribose at 25 °C.

be $K_{Ca-D-(-)-ribose} = 1.6$ and $K_{Ba-D(-)ribose} = 1.7$. By expressing each $K = 1 - \sigma/(\sigma^2 c)$, we have calculated σ and then $\theta = 2\sigma$c (Table 2).

Linear regression of τ_I^{-1} vs θ and of τ_{II}^{-1} vs ϕ according to eqs V and VI give k_1, k_{-1}, K_1, k_2, k_{-2}, and K_2 (Table 2), Figures 5 and 6. It is clear that K_1, K_2, and $K = K_1(1 + K_2)$ are in accord with literature data[8] for the overall complexation constants K of Ca^{2+} and Ba^{2+} with D-(−)-ribose at 25 °C. Further, k_1 and k_{-1} are close to each other for Ca^{2+} and Ba^{2+} interacting with D-(−)-ribose. However, the values of k_1 are below what one expects for a diffusion-controlled approach rate constant. According to Smoluchowski[9] $k_D = 8RT/3000\eta = 7.4 \times 10^9$ M^{-1} s^{-1}, where $R = 8.31 \times 10^7$ erg/K·mol is the gas constant and $\eta = 0.0089$ poise is the viscosity of water. That this first step of complexation involves more than diffusion is evidenced by the large differences in the μ_1 values. Evidently, partial cation desolvation, probably in the second coordination sphere water, is responsible for the above differences in the μ_1 values between Ca^{2+} and Ba^{2+}. From Table 1, at $c = 0.50$ mol/dm^3, one calculates for Ca^{2+} + D-(−)-ribose at 25 °C $\mu_1 = 93.7 \times 10^{-5}$, whereas, at the same concentration for Ba^{2+} + D-(−)-ribose at 25 °C, $\mu_1 = 454 \times 10^{-5}$, a factor of ∼5 larger. In the above $\mu_1 = (1/2)A_1 u f_R$. Also, the ratio between $k_2(Ba^{2+}) = 3.4 \times 10^8$ s^{-1} and $k_2(Ca^{2+}) = 7.3 \times 10^7$ s^{-1}, namely $k_2(Ba^{2+})/k_2(Ca^{2+}) = 4.7$, is within a factor of 2 of the ratios between the substitution rate constants of water in the first coordination sphere of the cations as reported in the literature.[7] The above differences (a factor of 2) should not surprise the reader, if one remembers that the above k_2 values refer to the removal of *three* molecules of water associated with the cation in the final complexes Ca^{2+}−ribose and Ba^{2+}−ribose according

to the literature, whereas the literature values of $k_{subs}(Ba^{2+})/k_{subs}(Ca^{2+}) \approx 10$ refer to monosubstituted complexes. It appears obvious that some cation size effect should appear in the complexation process.

One must specify that eq IV does not correspond *in all cases* to an S_N1 mechanism,[7] in the sense that k_2 is independent of the nature of the ligand, but only depends on the desolvation rate of the cation. In a previous paper,[1] we reported that Ca^{2+} + methyl-β-arabinopyranoside showed a relaxation process centered around ~41 MHz, whereas Ca^{2+} + 1,6-anhydro-β-glucopyranoside showed a relaxation process centered around ~26 MHz. These figures are different from the ones in Table 1 for Ca^{2+} + D-(−)-ribose, Ca^{2+} + D-(−)-lyxose, or Ca^{2+} + D-(−)-ribose, indicating a relaxation process centered around ~10 MHz. Evidently, the carbohydrate ligands participate, *in some cases*, in the activation energy profile of the complexation reaction.

Concern that the condition $k_1, k_{-1} \gg k_2, k_{-2}$ was not true for the case of Ba^{2+} +D-(−)-ribose prompted us to repeat the calculation using the more complete results of the Eigen−Tamm matrix analysis.[2] The sum S of the reverse relaxation times and the product P of the same two quantities, namely, $S = \tau_I^{-1} + \tau_{II}^{-1}$ and $P = \tau_I^{-1}\tau_{II}^{-1}$, in terms of the rate constants and θ are expressible as

$$S_{calc} = k_1\theta + k_{-1} + k_2 + k_{-2} \qquad \text{(VII)}$$

$$P_{calc} = k_1\theta(k_2 + k_{-2}) + k_{-1}k_{-2} \qquad \text{(VIII)}$$

Table IIIS (Supporting Information) reports the quantities S and P, both experimental and calculated, using the k and θ values reported above. It is shown that the agreement is within 30% for Ba^{2+} and within a few percent for Ca^{2+}, both figures within the experimental error of the quantity $(\tau_I^{-1}\tau_{II}^{-1})$.

Acknowledgment. The authors express thanks to Dr. Frieder Eggers and Mr. W. Sauermann for help in the construction of the kilohertz resonator cell that allowed us to extend the ultrasonic measurements below 1 MHz, down to ~80 kHz. Illustrations and several sugars were paid for by a grant from the Division of Chemical Sciences, Office of Basic Energy Science, Office of Science, U. S. Department of Energy.

Supporting Information Available: Experimental values of $S = \tau_I^{-1} + \tau_{II}^{-1}$ and $P = \tau_I^{-1}\tau_{II}^{-1}$ and calculated values of the same quantities according to eqs VII and VIII. This material is available free of charge via the Internet at http://pubs.acs.org.

References and Notes

(1) Cowman, M.; Eggers, F.; Eyring, E. M.; Horoszewski, D.; Kaatze, U.; Kreitner, U.; Petrucci, S.; Klöppel-Riech, M.; Stenger, J. *J. Phys. Chem. B* **1999**, *103*, 239.

(2) Eigen, M.; Tamm, K. *Z. Elektrochem.* **1962**, *66*, 93. Eigen, M.; Winkler, R. In *Neurosciences: Second Study Program*; Schmidt, F. O., Ed.; Rockefeller University Press: New York, 1970; pp 685−96.

(3) Stenger, J.; Cowman, M.; Eggers, F.; Eyring, E. M.; Kaatze, U.; Petrucci, S. *J. Phys. Chem. B* **2000**, *104*, 4782.

(4) Behrends, R.; Cowman, M.; Eggers, F.; Eyring, E. M.; Kaatze, U.; Majewski, J.; Petrucci, S.; Richmann, K. H.; Riech, M. *J. Am. Chem. Soc.* **1997**, *119*, 2182 and literature cited therein.

(5) Hemmes, P.; Fittipaldi, F.; Petrucci, S. *Acustica* **1969**, *21*, 228.

(6) For a review, see: Farber, H.; Petrucci, S. In *Chemical Physics of Solvation*; Dogonadze, R. R., et al., Eds.; Elsevier: Amsterdam, 1986; Part B.

(7) Basolo, F.; Pearson, R. G. *Mechanism of Inorganic Reactions*, 2nd ed; John Wiley and Sons: New York, 1967; p 155.

(8) Goulding, D. J. *J. Chromatogr.* **1975**, *103*, 229.

(9) von Smoluchowski, M. *Z. Phys. Chem.* **1917**, *92*, 129. For a review, see: Petrucci, S. *Ionic Interactions*; Academic Press: New York, 1971; Vol. II, Chapter 7.